Article No. mb981890 J. Mol. Biol. (1998) 280, 913–923

JMB

Substrate Assistance in the Mechanism of Family 18 Chitinases: Theoretical Studies of Potential Intermediates and Inhibitors

Ken A. Brameld[1,2], William D. Shrader[2], Barbara Imperiali[2] and William A. Goddard III[1,2]*

[1]*Materials and Process Simulation Center Beckman Institute (139-74)*

[2]*Division of Chemistry and Chemical Engineering California Institute of Technology, Pasadena CA 91125, USA*

*Corresponding author

Based on first principles and molecular mechanics calculations, we conclude that the mechanism of hevamine (a family 18 chitinase) involves an oxazoline ion intermediate stabilized by the neighboring C2′ acetamido group. In this intermediate, the acetamido carbonyl oxygen atom forms a covalent bond to C1′ of *N*-acetyl-glucosamine and has a transferred positive charge from the pyranose ring onto the acetamido nitrogen atom, leading to an anchimeric stabilization of 38.1 kcal/mol when docked with hevamine.

This double displacement mechanism involving an oxazoline intermediate distinguishes the family 18 chitinase (which have one acidic residue near the active site) from family 19 chitinase and from hen egg-white lysozyme, which have two acidic residues near the active site.

The structural and electronic properties of the oxazoline intermediate are similar to the known chitinase inhibitor allosamidin, suggesting that allosamidins act as transition state analogs of an oxazoline intermediate. Structural and electronic features of the oxazoline ion likely to be important in the design of new chitinase inhibitors are discussed.

Introduction

Chitinases catalyze the hydrolysis of chitin, a β(1,4)-linked *N*-acetyl-glucosamine (GlcNAc) polysaccharide (Figure 1), and are critical for the normal development of insects (Fukamizo & Kramer, 1995) and fungi (Bartnicki-Gracia, 1968). Structurally diverse chitinases have been isolated from plants, where they may act as a defense against fungal pathogens (Boller *et al.*, 1983; Collinge *et al.*, 1993). The five known classes of chitinases are grouped into two glycosyl hydrolase families (Henrissat & Bairoch, 1993). Family 18 consists of class III and class V chitinases found in a wide range of organisms including bacteria, plants, animals and fungi. Family 19 consists of class I, II and IV chitinases, and are found only in plants. The enzyme structures and hydrolysis mechanisms for the two families appear to be quite different. A knowledge of the reaction mechanism is important for the design of new transition state analogs, which may act as chitinase inhibitors and potential insecticides (Sakuda *et al.*, 1986; Koga *et al.*, 1987) or fungicides (Schlumbaum *et al.*, 1986).

Here, we use first principles methods and molecular mechanics modeling to examine the reaction mechanism for hevamine, a family 18 chitinase. First we used *ab initio* quantum mechanics (QM) to study (in both the gas and solution phases) three possible intermediates formed during the enzymatic hydrolysis of chitin (**1** to **3**, Figure 2A). Second, we developed a force-field (FF) that correctly describes the structure and energy differences between these three intermediates for use in molecular dynamics (MD) studies. We then used this FF to examine the structures of these three intermediates (with a $(GlcNAc)_2$ disaccharide substitution at O4′ (**4** to **6**, Figure 2A)), bound to the active site of hevamine, a family 18 chitinase. Finally, these structure were used for single point QM energy calculations including the effects of the enzyme active site and solvation. These results support the intermediacy of an oxazoline species in the reaction mechanism. Such a mechanism differs

Abbreviations used: FF, force-field; GEWL and HEWL, goose and hen egg-white lysozyme, respectively; MD, molecular dynamics; RMS, root-mean-square; QM, quantum mechanics.

0022–2836/98/300913–11 $30.00/0

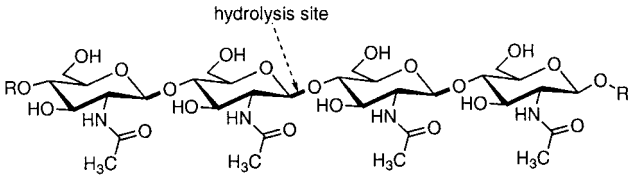

Figure 1. An arrow marks the hydrolysis site of chitin, the β(1,4)-*N*-acetyl-glucosamine (GlcNAc) polysaccharide substrate of chitinases.

substantially from that of the family 19 chitinases and hen egg-white lysozyme (the best studied glycosyl hydrolase).

We also find the electrostatic potential surfaces of the hevamine-bound oxazoline intermediate and allosamidin, a potent chitinase inhibitor (Sakuda *et al.*, 1986; Kinoshita *et al.*, 1993), to be quite similar, supporting the proposal that the allosamidins act as transition state analogs (Terwisscha van Scheltinga *et al.*, 1995).

The section on Review of Mechanistic Understanding discusses the current understanding of the chitinase hydrolysis mechanisms and Calculations covers the computational details. The Results and Discussion report the results of our calculations on the hydrolysis reaction intermediates and discusses implications for understanding the mechanism of action of known inhibitors.

Review of Mechanistic Understanding

Extensive studies of the mechanism of hen egg-white lysozyme (HEWL) show that glycoside hydrolysis requires two acidic residues (Glu36 and Asp52), one of which is protonated (Phillips, 1967). The consensus view (Sinnot, 1990) of the mechanism (Scheme 1) involves protonation of the β-(1,4)-glycosidic oxygen atom, leading to an oxocarbenium ion intermediate, which is stabilized by the secondary carboxylate group (either through covalent or electrostatic interactions). Nucleophilic attack by water yields the hydrolysis product, which necessarily retains the initial anomeric configuration. This is commonly referred to as the double displacement mechanism of hydrolysis (Koshland, 1953; Sinnot, 1990; Davies & Henrissat, 1995).

The X-ray crystal structure of a family 19 chitinase isolated from barley shows structural similarities with HEWL, suggesting an analogous double displacement mechanism (Hart *et al.*, 1995). However, subsequent analysis of the anomeric products for two family 19 chitinases show that an inversion of the anomeric configuration accompanies these reactions (Fukamizo *et al.*, 1995; Iseli *et al.*, 1996). This observation rules out the double displacement mechanism of HEWL. A possible mechanism explaining inversion is a concerted single displacement reaction (McCarter & Withers, 1994; Davies & Henrissat, 1995) in which a bound water molecule acts as the nucleophile. Although this water molecule was not observed in the crystal structure, the second catalytic carboxylate group is at a sufficient distance to allow coordination of a

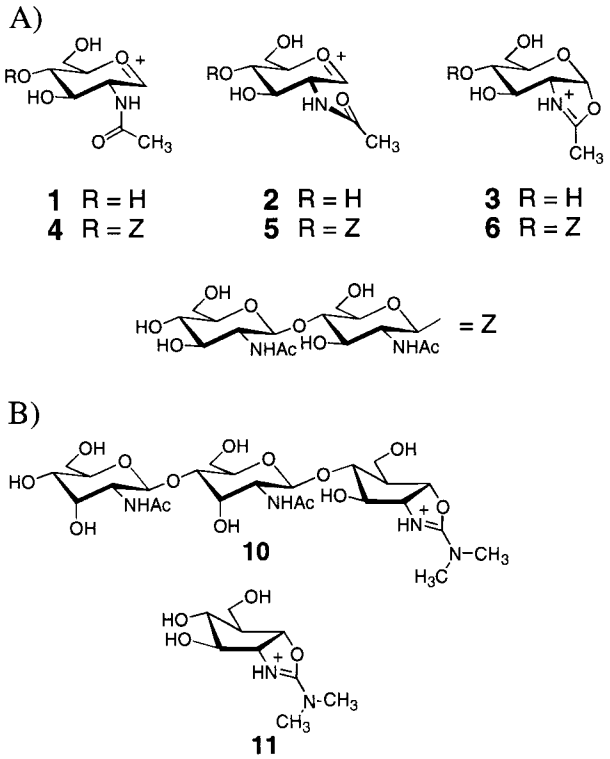

Figure 2. A, Three putative transition states involved in the chitinase hydrolysis mechanism were examined. **1** and **4** are the oxocarbenium species with an extended *N*-acetyl geometry; **2** and **5** have a rotated *N*-acetyl geometry; **3** and **6** are the global, minimum oxazoline ion structures. B, Allosamizoline (**11**) is the aglycone of allosamidin (**10**), a potent chitinase inhibitor.

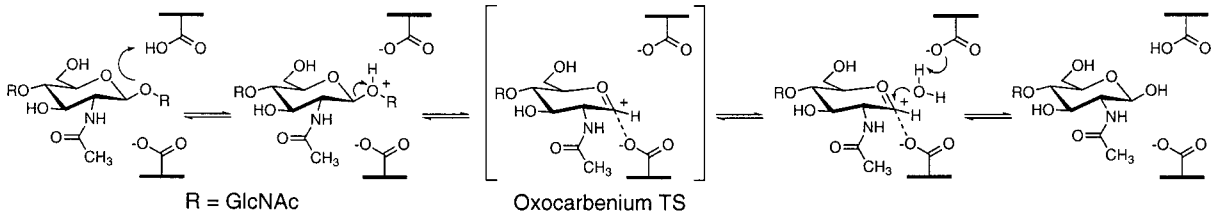

Scheme 1. The double-displacement mechanism of lysozyme.

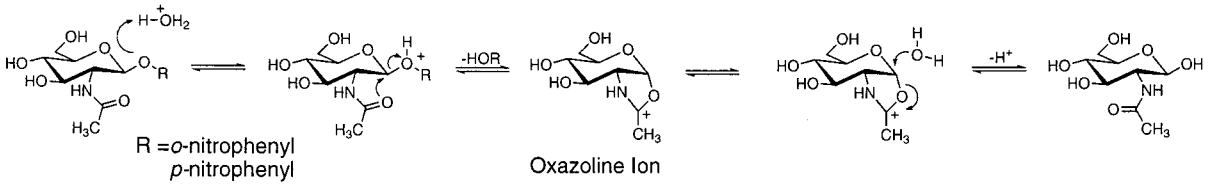

Scheme 2. The proposed anchimeric assisted mechanism of spontaneous hydrolysis of *o* and *p*-nitrophenyl 2-acetamido-2-deoxyglucopyranosides (Piszkiewiez & Bruice, 1967, 1968).

water molecule, consistent with a single displacement mechanism (Hart *et al*., 1995).

Crystallographic analysis of family 18 chitinases isolated from both bacteria (Perrakis *et al*., 1994) and plants (Terwisscha van Scheltinga *et al*., 1994, 1996) reveal a common structural motif within two short homologous sequences. Thus, the family 18 chitinases share a similar active site, located at the carboxy terminus and comprising a $(\beta\alpha)_8$-barrel domain. Hydrolysis has been reported to proceed with retention of the anomeric configuration (Phillips, 1967; Armand *et al*., 1994), consistent with the double displacement hydrolysis mechanism, as in HEWL. However, for hevamine and other family 18 chitinases, the three-dimensional structure clearly shows only one acidic residue in the active site (Terwisscha van Scheltinga *et al*., 1996). Thus, there must be an alternative mechanism that allows a double displacement reaction to take place, yet stabilizes the oxocarbenium ion intermediate without requiring a second carboxylate residue.

The spontaneous acid-catalyzed hydrolysis of 2-acetamido-substituted polysaccharides in solution has been reported to occur through anchimeric assistance by the acetamido carbonyl group of a GlcNAc residue (Piszkiewiez & Bruice, 1967, 1968; and Scheme 2). It was proposed that anchimeric participation may play a role in the enzymatic mechanism of lysozyme (Lowe *et al*., 1967). This proposal was later disproved for HEWL by mutagenesis studies, which indicate that two acidic residues are essential for enzyme activity (Parsons & Raferty, 1969). However, such a mechanism could conceivably be operative for the family 18 chitinases (Van Vranken, 1992; Davies & Henrissat, 1995; Terwisscha van Scheltinga *et al*., 1995), goose egg-white lysozyme (GEWL; Grütter *et al*., 1983; Weaver *et al*., 1995), and soluble lytic transglycosylase (Thunnissen *et al*., 1994, 1995). Experimental evidence in support of the anchimeric assistance mechanism is provided by the crystal structure of the inhibitor allosamidin (**10**) bound to the active site of hevamine (Terwisscha van Scheltinga *et al*., 1995), where the possibility of ''anchimeric assistance by the [C2′] *N*-acetyl'' group is suggested. Such C2′ acetamido participation would offer a simple mechanistic alternative (Scheme 3) for hydrolysis by the family 18 enzymes, which lack a second active site carboxylate group capable of stabilizing an oxocarbenium ion.

In order to determine whether anchimeric stabilization is significant in the enzymatic hydrolysis of chitin, we carried out *ab initio* QM calculations (Greeley, 1994; Muller *et al*., 1994; Murphy *et al*., 1994; Langlois *et al*., 1994), including solvation (Tannor *et al*., 1994), on possible intermediates. We then developed a FF able to reproduce the energetics and relative energies obtained from QM and used this to predict the structure and energetics of $(GlcNAc)_2$ disaccharide substituted intermediates (**4** to **6**) at the active site of hevamine. Single point *ab initio* QM energies (with or without solvent) of the aglycone intermediates bound to the active site were similar to those calculated for the solvated isolated intermediates, clearly showing that the lowest energy intermediate is the oxazoline species **3**. Here the acetamido carbonyl oxygen atom forms a covalent bond to C1′ of *N*-acetyl-glucosamine, which transfers the positive charge from the pyranose ring onto the acetamido nitrogen atom. Structural and electronic features that may be important in the rational design of second generation inhibitors are discussed below.

Calculations

The *ab initio* QM calculations (HF/6-31G**) were carried out with the PS-GVB 2.24 program (Greeley *et al*., 1994; Muller *et al*., 1994; Murphy

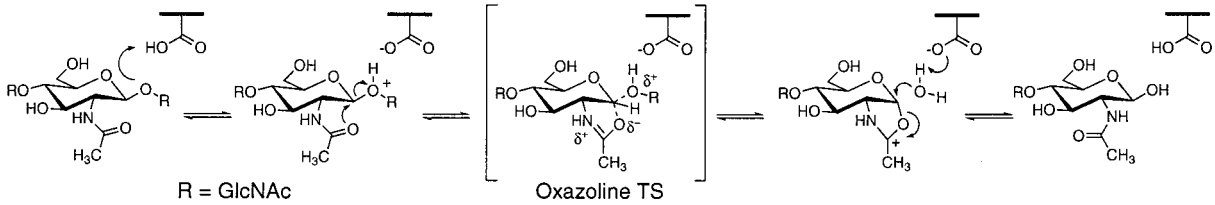

Scheme 3. The proposed mechanism for chitinase involving an oxazoline ion intermediate.

et al., 1994; Langlois *et al.*, 1994; Tannor *et al.*, 1994) from Schrödinger, Inc. Initial geometries of **1** to **3** were obtained using the Dreiding FF (Mayo *et al.*, 1990) with the PolyGraf MD program, which is distributed by Molecular Simulations Inc., San Diego. The geometry was then optimized using QM. No constraints were placed on **1** or **3**. However, to determine the energetic effects of anchimeric stabilization, the C-N-C2′-C3′ torsion angle of **2** was constrained to 68.5°. This torsion angle was chosen because it is a local minimum determined from the unconstrained geometry optimization of **3**. Solvent polarization was included self-consistently in the QM wavefunction using the Poisson-Boltzmann continuum description ($\varepsilon = 80.37$) outside the solvent-accessible surface (probe radius 1.2 Å; Tannor *et al.*, 1994). The geometry optimizations were carried out in the gas phase. For **3**, we also optimized the geometry while simultaneously including the forces due to solvation; however, these calculations found the change in geometry to be insignificant (RMS coordinate difference 0.03 Å).

Atomic point charges were determined (Muller *et al.*, 1994; Murphy *et al.*, 1994; Langlois *et al.*, 1994) from the electrostatic potential derived from the electron density distribution (constrained to reproduce the molecular monopole and dipole moments) calculated from the converged wavefunctions. Electrostatic potential surfaces were calculated and displayed using the PS-GVB output with the Spartan 4.1.2 visualizer, distributed by Wavefunction Inc., Irvine, CA.

MD studies for the isolated intermediates were carried out with the Dreiding FF (Mayo *et al.*, 1990) using the PolyGraf molecular modeling program. A standard coulomb potential was used with no distance-dependent dielectric and all non-bond interactions considered explicitly. The O_2 atom type van der Waals radius was reduced to 3.00 Å, all other parameters were unchanged.

The starting structures for the $(GlcNAc)_2$ disaccharide of intermediates **4** to **6** were taken from the allosamidin/hevamine crystal structure and merged with the aglycone intermediates **1** to **3**. Docking of these glycosylated intermediates with hevamine was achieved in a three-step process using PolyGraf. First, a least-squares alignment was carried out matching the oxazoline **6** and constrained oxocarbenium ion **5** intermediates with the allosamidin/hevamine complex. The allosamidin was then deleted from the structure, leaving only the docked intermediates. In the case of the extended *N*-acetyl geometry of **4**, annealing simulations using MD were carried out to determine the optimum binding position.

QM-derived charges were used for the intermediates (Figure 3) and the default Charmm charges invoked with the Dreiding FF were used for hevamine. The total charge within the active site was zero with a net charge of +1 on each intermediate and −1 on Asp125. A spline cutoff of 13.5 Å was used for the non-bond terms.

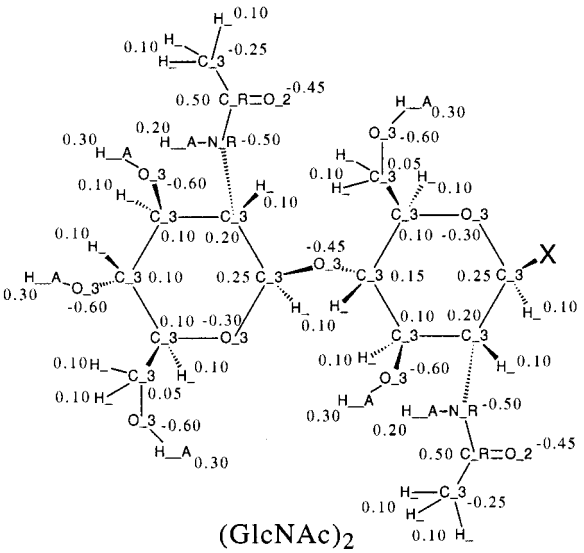

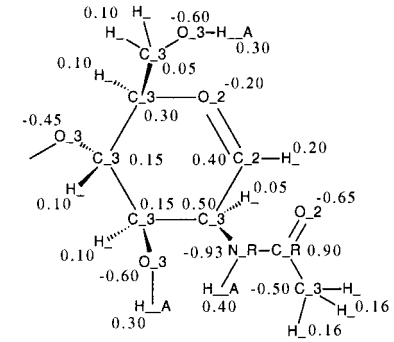

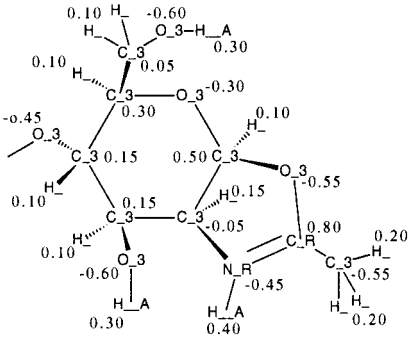

Figure 3. Charges and FF atom types used for MD calculations of intermediates **4** to **6**.

A series of ten cycles of MD quenching simulations from 50 to 300 K for 2 ps each was carried out for each intermediate. For the first five cycles, the enzyme was fixed in the crystallographic conformation. For the remaining five cycles, the five active site residues (Asp125, Glu127, Gln181, Tyr183 and Trp255) were allowed to relax in addition to the intermediates. Energy minimization

of the annealed structure yielded the final docked conformations. Coordinates obtained from these structures optimized with the FF were used for the *ab initio* QM calculations (HF/6-31**). These clusters (**7** to **9**) included the hydrogen-terminated side-chains of residues Asp125, Glu127, Gln181, Tyr183 and Trp255 (see Figure 5).

Results and Discussion

Energetics of hydrolysis intermediates

To explore the possibility that an oxocarbenium ion intermediate may be internally stabilized by the acetamido carbonyl group of GlcNAc residue, we carried out QM calculations on a C1′-deoxy-*N*-acetyl-glucosamine ion. The global energy minimum leads to the oxazoline species, **3**, in which the acetamido carbonyl group rotates towards C1′, forming a covalent bond (Figure 2). In order to determine the magnitude of this stabilization, we also examined two conformations (**1** and **2**) with the orientation of this internal carbonyl group either extended or constrained by fixing the C-N-C2′-C3′ torsion angle and optimizing the remainder of the structure. Conformation **1** is extended and has the carbonyl group away from the active site, while conformation **2** orients the carbonyl group to be parallel with and below the plane of the hexose ring, enabling it to interact with the positive O5′ without forming a covalent bond. Table 1 lists the relative energies for each conformation in the gas phase and solvated in water (using the Poisson-Boltzmann continuum solvent approximation in conjunction with the solvent-accessible surface; Tannor *et al*., 1994).

We find conformation **2** to be 16.9 kcal/mol higher in energy than the oxazoline ion, while the extended conformation is 21.7 kcal/mol higher in energy. (These values are with solvation, the gas phase values are 16.1 and 29.8 kcal/mol, respectively.) Thus, anchimeric stabilization is a significant force in making the oxazoline ion a thermodynamically accessible intermediate in solution. These results are consistent with the experimental observation that anchimeric assistance occurs during spontaneous hydrolysis of 2-acetamido substituted polysaccharides (Piszkiewiez & Bruice, 1967, 1968).

Table 1. Relative energies of hydrolysis intermediates (kcal/mol)

Conformation	Gas phase	HF/6-31G** Solvated[a]	DREIDING[b]
1	21.6	20.0	20.5
2	15.6	16.9	16.5
3	0.0[c]	0.0[d]	0.0[e]

[a] Solvation energy calculated (Tannor *et al*., 1994) using a Poisson-Boltzmann continuum description ($\varepsilon = 80.37$) outside the solvent-accessible surface (probe radius 1.2 Å).
[b] Molecular mechanics energy calculated with the Dreiding FF (Mayo *et al*., 1990).
[c] Total energy = −739.66680 hartrees.
[d] Calculated solvation energy = 70.3 kcal/mol.
[e] Total energy = 18.06 kcal/mol.

It is conceivable that the enzymatic hydrolysis mechanism of β(1,4)-linked C2′-*N*-acetyl-polysaccharides could still proceed through an oxocarbenium ion if there was sufficient electronic stabilization within the enzyme active site. Theoretical studies have shown that local electrostatic factors are important for lysozyme, which has an asymmetric charge distribution (Warshel & Levitt, 1976). Electrodynamics calculations (Dao-Pin *et al*., 1988) for the lysozyme active site reveal a large induced electric field, which was proposed to stabilize bond cleavage and the resulting charge separation. Hevamine and other family 18 chitinases differ from lysozyme by having only one acidic residue capable of charge stabilization in the active site. Nevertheless, the possibility of electrostatic stabilization of an oxocarbenium ion when bound to a family 18 chitinase (in vacuum and solvated) was explored. As expected, no such stabilization was observed due to the lack of local charged groups capable of stabilizing the positive oxocarbenium ion.

We examined the extent of enzymatic stabilization induced by hevamine using a combination of molecular mechanics and *ab initio* QM calculations (HF/6-31G**). Using the Dreiding FF (Mayo *et al*., 1990), it was first established that the gas phase molecular mechanics structures and relative energies for each intermediate (**1** to **3**) were consistent with those obtained using QM. The molecular mechanics energies are listed in Table 1 and show good agreement (within 1 kcal/mol) with the QM results. The RMS difference in coordinates between structures determined with the two methods was only 0.16 and 0.10 Å for conformations **1** and **3**, respectively. The constrained conformation **2** had a larger RMS coordinate difference (0.31 Å) primarily due to the non-planar C2′ *N*-acetyl nitrogen atom, which was not reproduced by molecular mechanics.

Each of the three possible $(GlcNAc)_2$ disaccharide substituted intermediates was aligned with the allosamidin/hevamine complex crystal structure. These docked conformations served as starting points for a series of MD and energy minimization cycles. Initially, the entire enzyme was held fixed in the crystal structure geometry. For the final series of quenched dynamics cycles, the five residues (Asp125, Glu127, Gln181, Tyr183 and Trp255) forming the active site binding pocket were free to move.

The results of these MD simulations are consistent with simulations of the isolated intermediates. The lowest-energy structure remains the oxazoline ion, with the constrained oxocarbenium ion lying 7.5 kcal/mol higher in energy. The extended *N*-acetyl geometry is much less favorable than the oxazoline ion with an energy difference of 31.8 kcal/mol. The optimum structures from these

MD simulations were used for more detailed QM calculations. Each amino acid side-chain that forms part of the active site binding pocket was then terminated with a hydrogen atom in place of the alpha carbon atom. This reduced system served as a model for which single point energy calculations, both in the gas phase and solvated in water, were carried out, which included the effects of enzymatic stabilization.

Molecular mechanics and *ab initio* QM (HF/6-31G**) single point energies were calculated for model systems **7** to **9** (see Figure 5). Table 2 lists the energies for each cluster. Molecular mechanical methods gave the correct ordering of the three intermediates when compared to the QM results. Both methods clearly indicate that there is no enzymatic stabilization of oxocarbenium ion **1** over the oxazoline ion intermediate. In all environments examined (gas phase, solvated, gas phase/bound to hevamine and solvated/bound to hevamine). The oxocarbenium ion intermediate is 21.6, 20.0, 38.1 and 41.3 kcal/mol higher in energy than the oxazoline intermediate. Indeed, in the presence of the active site residues, the oxocarbenium ion with an extended *N*-acetyl geometry is destabilized relative to the other conformations.

In the calculations discussed above, we have not explored the formation of each of the different intermediates from the protonated chitin substrate. Rather, we have started with the assumption that glycosidic bond cleavage (the first step in any glycosidic hydrolysis mechanism) will result in a charged intermediate. The energetics of glycosidic bond cleavage and the barriers to formation of an oxocarbenium ion and oxazoline ion will be addressed elsewhere (Brameld & Goddard, 1998).

Structural and electronic properties of intermediates

Analysis of the structural and electronic properties of the three putative intermediates reveals interesting differences important for the design of transition state analogs that may act as inhibitors. Bond lengths, angles and torsions for the hexose ring (Figure 4) of conformations **1** and **3** are given in Table 3. The complete set of Cartesian coordinates for optimized structures **1** and **3** are available as supplementary material.

Conformations **1** and **2** have an sp^2 C1′ center, forcing the hexose ring to adopt a more planar

Table 2. Relative energies of hydrolysis intermediates explicitly including hevamine active site residues (kcal/mol)

Conformation	DREIDING[a]	HF/6-31G**	HF/6-31G** solvated
4	21.4	38.1	41.3
5	12.5	16.2	23.3
6	0.0[b]	0.0[c]	0.0[d]

[a] Molecular mechanics energy calculated with the Dreiding FF (Mayo *et al.*, 1990).
[b] Total energy = −130.4 kcal/mol.
[c] Total energy = −2069.82945 hartrees.
[d] Total solution phase energy = −2069.91545 hartrees.

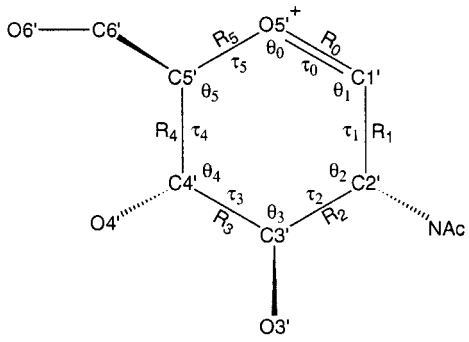

Figure 4. Atom numbering and definition of geometric parameters for the oxocarbenium ion.

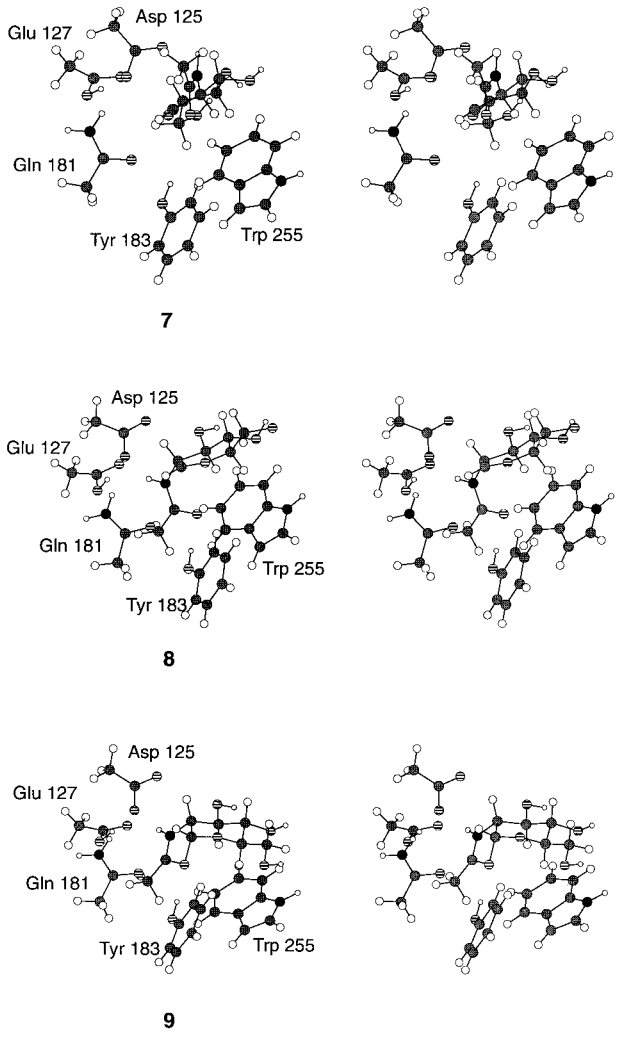

Figure 5. Stereo views of the clusters used for quantum mechanical calculations including the hevamine active site residues. Dotted atoms are carbon, hatched are oxygen, filled are nitrogen and white are hydrogen. Here **7**, **8** and **9** correspond to **1**, **2** and **3** of Figure 2A.

Table 3. Energy optimized geometrical parameters for the hexose ring of the oxocarbenium ion (**1**) and oxazoline ion (**3**)

Parameter[a]	Oxocarbenium ion (**1**) Gas phase	Oxazoline ion (**3**) Gas phase	Oxazoline ion (**3**) Solvated
R_0 (C1′-O5′)[b]	1.231	1.338	1.349
R_1 (C1′-C2′)	1.502	1.537	1.537
R_2 (C2′-C3′)	1.524	1.529	1.530
R_3 (C3′-C4′)	1.524	1.522	1.521
R_4 (C4′-′)	1.528	1.527	1.526
R_5 (C5′-O5′)	1.494	1.437	1.431
θ_0 (C5′-O5′-C1′)[c]	126.4	120.5	120.0
θ_1 (O5′-C1′-C2′)	123.5	117.8	118.0
θ_2 (C1′-C2′-C3′)	109.6	114.5	114.4
θ_3 (C2′-C3′-C4′)	108.9	110.8	110.0
θ_4 (C3′-C4′-C5′)	110.3	108.1	107.9
θ_5 (C4′-C5′-O5′)	110.8	107.9	108.2
τ_0 (C5′-O5′-C1′-C2′)[c]	−5.4	−35.2	−33.1
τ_1 (O5′-C1′-C2′-C3′)	24.9	25.5	25.2
T_2 (C1′-C2′-C3′C4′)	−52.0	−37.5	−39.1
τ_3 (C2′-C3′-C4′-C5′)	62.2	57.0	59.1
τ_4 (C3′-C4′-C5′-O5′)	−41.3	−63.5	−64.6
T_5 (C4′-C5′-O5′-C1′)	13.4	54.3	52.7

[a] See Figure 4 for atom numbering and definitions of geometric parameters.
[b] Bond lengths in Å.
[c] Bond angles and torsions in degrees.

half-chair geometry. In contrast, the oxazoline ion (**3**) maintains a mildly distorted full chair conformation, since all atoms of the hexose ring have sp^3 hybridization. This is evident by comparing the C5′-O5′-C1′-C2′ torsion angle (τ_0) of each conformation. The more planar oxocarbenium ion **1** has a torsion angle of −5.4°, while the oxazoline ion is puckered to −35.2°. The O5′-C1′ bond length is 1.23 Å for **1** and **2**, indicating a double bond order. This is consistent with the longer O5′-C1′ bond length of 1.34 Å for **3** and the bond length of 1.49 Å for the newly formed bond between C1′ and the *N*-acetyl carbonyl oxygen atom.

The electrostatic potential surfaces for intermediates **1** and **3** are shown in Figure 6. For the oxocarbenium ion, **1**, a localized positive charge density is observed on C1′ and O5′ as expected. For the more stable oxazoline ion, **3**, the charge is transferred to the protonated oxazoline, formed upon cyclization of the *N*-acetyl group. This migration alters the electrostatic potential surface of the entire hexose ring, allowing greater delocalization of the positive charge (now distributed between the N, C and O atoms of the *N*-acetyl group).

Transition state inhibitors

The mechanism of HEWL involves an oxocarbenium ion intermediate, stabilized by a second carboxylate group in the enzyme active site

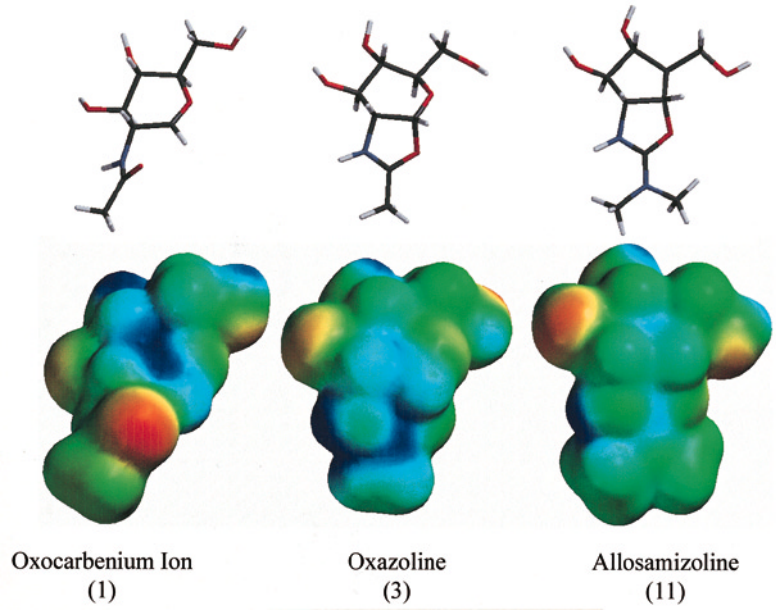

Figure 6. Electrostatic potential surfaces of the oxocarbenium (**1**) and oxazoline (**3**) intermediates compared to inhibitors allosamizoline (**11**). Red indicates a negative potential and blue a positive potential.

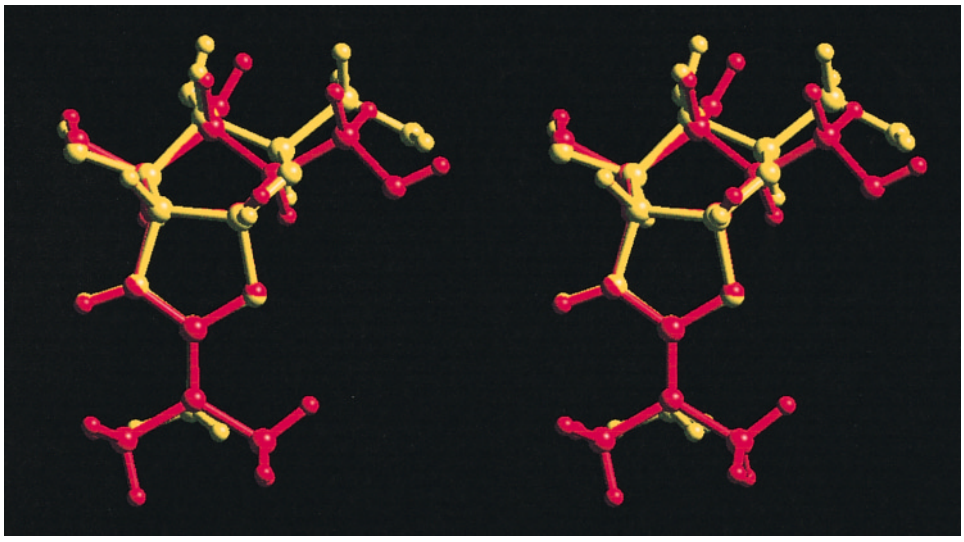

Figure 7. A stereo view of the optimized oxazoline ion intermediate **3** (yellow) overlaid with the optimum allosamizoline structure (red).

(Koshland, 1953; Phillips, 1967; Sinnot, 1990; McCarter & Withers, 1994; Davies & Henrissat, 1995). Lactones have been reported to act as lysozyme inhibitors by mimicking the electronic and structural characteristics of the oxocarbenium ion intermediate (Ford *et al.*, 1974). Unique properties of the oxocarbenium ion (**3**) include a planar region of the hexose ring and a localized positive charge near C1′ and O5′. By analogy, a compound with structural and electronic properties mimicking the oxazoline intermediate would be expected to act as an inhibitor of the family 18 chitinases (assuming the oxazoline ion intermediate to be involved in the mechanism).

Allosamidin, **10** (Figure 2B), and related natural products are pseudotrisaccharide chitinase inhibitors (Sakuda *et al.*, 1986) isolated from the mycelium of *Streptomyces* sp. Although detailed inhibition and kinetics studies have not been reported, allosamidin is believed to act as a transition state analog (Van Vranken, 1992; Terwisscha van Scheltinga *et al.*, 1995; Robertus *et al.*, 1995). Moreover, allosamidin shows no inhibitory activity against lysozyme (Koga *et al.*, 1987), which is consistent with the suggestion that the two enzymes have different mechanisms (and therefore unique transition states) for hydrolysis. It was originally proposed that the planar protonated oxazoline ring acts as an oxocarbenium ion transition state analog (Robertus *et al.*, 1995). However, an X-ray structure of hevamine with allosamidin bound in the active site (Terwisscha van Scheltinga *et al.*, 1995) led to the suggestion that allosamizoline (**11**), the aglycone portion of allosamidin, instead resembles an oxazoline ion reaction intermediate.

We carried out QM calculations (at the same level as for the chitinase reaction intermediates **1** to **3** and without constraints) to optimize the geometry of allosamizoline (**11**; Figure 2B). This aglycone allosamidin derivative has a hydroxyl substitution for the *N*-acetyl-glucosamine disaccharide of allosamidin (**10**), thus allowing a comparison with intermediates **1** to **3**. The optimized geometry and electrostatic potential surface is shown in Figure 6. An overlay of the oxazoline ion intermediate and allosamizoline (Figure 7) shows the striking match between the two structures particularly in the charged region of the acetamido group. Indeed, the RMS coordinate difference between equivalent non-hydrogen atoms is 0.21 Å. To carry out this RMS match calculation, the following atoms from oxazoline ion were not included: O5′, C5′, C6′ and O6′; and from allosamizoline: atoms equivalent to C5′, C6′ and the dimethyl portion of the amine.

The electrostatic potential surfaces of allosamizoline and putative chitinase reaction intermediates **1** to **3** (Figure 6), indicate clearly that the electronic properties of allosamizoline (**11**) are similar to those of the oxazoline intermediate (**3**) and dissimilar to the oxocarbenium ion (**1**). Both **3** and **11** have a localized positive charge density on the oxazoline ion. In contrast, oxocarbenium ion **1** has a localized positive charge between O5 and C1. Enzymatic stabilization of these two species (**1** and **3**) would require different active site structures and electrostatic properties. For **1**, the active site would need acidic residues adjacent to the oxazoline, whereas for **3** the acidic residues would need to be on the opposite side of the binding cleft to stabilize the oxocarbenium ion.

Indeed, an analysis of the electrostatic potential surface of the enzyme active site model (Figure 8) reveals a large negatively charged region opposite the oxazoline moiety. In addition, visualization of the complementary electrostatic potential surface of the oxazoline intermediate shows great similarity between the enzymatic surface and the oxa-

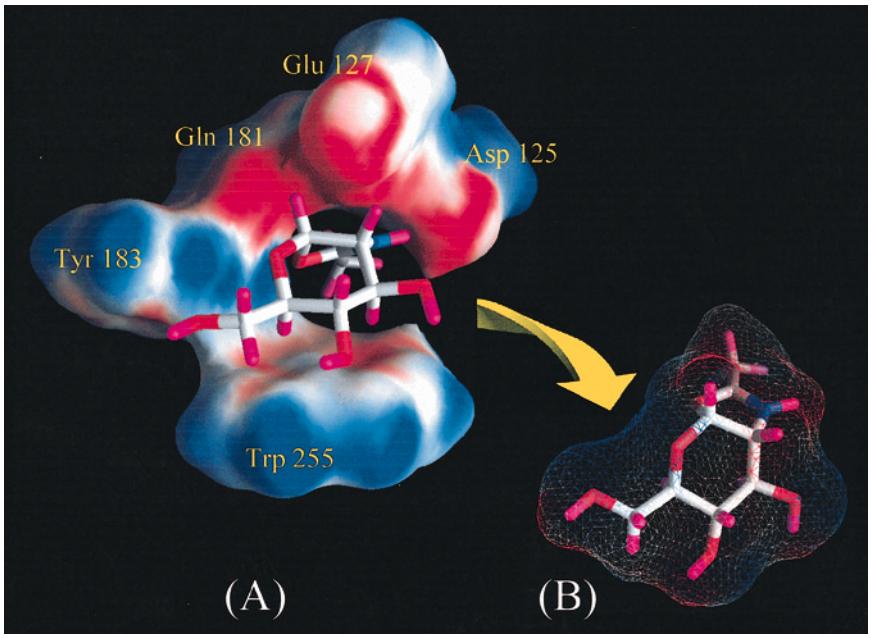

Figure 8. (A) Electrostatic potential surface of the hevamine active site model cluster (**9**). (B) Complementary electrostatic surface (shown as a grid) of the oxazoline intermediate. Red denotes a negative potential and blue a positive potential.

zoline surface. It is evident that the charge distribution within the enzyme active site cannot stabilize an oxocarbenium ion intermediate and this likely results in the observed destabilization of this species.

Conclusions

Using *ab initio* quantum mechanical calculations, we examined intermediates for the enzymatic hydrolysis of chitin. We find that the oxazoline ion intermediate is stabilized by the C2′ acetamido group, both in an isolated system and bound to hevamine. Similar calculations on a known inhibitor belonging to the allosamidin family of natural products revealed structural and electronic similarities between this inhibitor and the oxazoline ion intermediate. Our calculations lend strong theoretical support to the increasing body of experimental evidence (Sakuda *et al.*, 1986; Terwisscha van Scheltinga *et al.*, 1995) which suggests that the mechanism of family 18 chitinases involves anchimeric assistance stabilizing an oxazoline ion reaction intermediate.

The double displacement mechanism involving an oxazoline intermediate may not be unique to the chitinases. Other enzymes have been identified that hydrolyze β(1,4)-linked C2′-*N*-acetylpolysaccharides but are also missing a second acidic residue. These include GEWL (Grütter *et al.*, 1983; Weaver *et al.*, 1995) and the soluble lytic transglycosylase (Thunnissen *et al.*, 1994, 1995). These enzymes may utilize the same oxazoline ion intermediate by anchimeric stabilization.

The oxazoline intermediate state serves as a target for the rational design of more potent glycosidase inhibitors specific to family 18 chitinases. Simple analogs of allosamidin that incorporate the key features of a delocalized positive charge while maintaining a chair-like sugar conformation may prove to be synthetically more accessible than allosamidin itself. Such analogs could lead to a new generation of chitinase inhibitors.

Acknowledgments

This research was funded by DOE-BCTR (DE-FG36-93CH105 81, David Boron). Facilities of the MSC are also supported by grants from NSF (CHE 95-22179 and ASC 92-100368), Chevron Petroleum Technology Co., Aramco, Asahi Chemical, Owens-Corning, Chevron Chemical Company, Asahi Glass, Chevron Research and Technology Co., Hercules, BP Chemical, and Beckman Institute. Some calculations were carried out at the NSF San Diego Supercomputer Center (SDSC) and on the JPL Cray.

References

Armand, S., Tomita, H., Heyraud, A., Gey, C., Watanabe, T. & Henrissat, B. (1994). Stereochemical course of the hydrolysis reaction catalyzed by chitinases A1 and D from *Bacillus circulans* WL-12. *FEBS Letters*, **343**, 177–1180.

Bartnicki-Gracia, S. (1968). Cell wall chemistry, morphogenesis, and taxonomy of fungi. *Annu. Rev. Microbiol.* **22**, 87–108.

Boller, T., Gehri, A., Mauch, F. & Vogeli, U. (1983). Chitinase in bean leaves; induction by ethylene, purification, properties, and possible function. *Planta,* **157**, 22–31.

Brameld, K. A. & Goddard, W. A., III (1998). Substrate distortion to a boat conformation at subsite −1 is critical in the mechanism of family 18 chitinases. *J. Am. Chem. Soc.* **120**, 3571–3580.

Collinge, D. B., Kragh, K. M., Mikkelsen, J. D., Nielsen, K. K., Rasmussen, U. & Vad, K. (1993). Plant chitinases. *Plant J.* **3**, 31–40.

Dao-Pin, S., Liao, D. & Remington, S. J. (1989). Electrostatic fields in the active site of lysozymes. *Proc. Natl Acad. Sci. USA,* **86**, 5361–5365.

Davies, G. & Henrissat, B. (1995). Structures and mechanisms of glycosyl hydrolases. *Structure,* **3**, 853–859.

Ford, L. O., Johnson, L. N., Machin, P. A., Phillips, D. C. & Tjian, R. (1974). Crystal structure of a lysozyme-tetrasaccharide lactone complex. *J. Mol. Biol.* **88**, 349–371.

Fukamizo, T. & Kramer, K. J. (1985). Mechanism of chitin hydrolysis by the binary chitinase system in insect moulting fluid. *Insect Biochem.* **15**, 141–145.

Fukamizo, T., Koga, D. & Goto, S. (1995). Comparative biochemistry of chitinases – anomeric form of the reaction-products. *Biosci. Biotech. Biochem.* **59**, 311–313.

Greeley, B. H., Russo, T. V., Mainz, D. T., Friesner, R. A., Langlois, J.-M., Goddard, W. A., III, Donnelly, R. E. & Ringnalda, M. N. (1994). New pseudospectral algorithms for electronic-structure calculations – length scale separation and analytical 2-electron integral corrections. *J. Chem. Phys.* **101**, 4028–4041.

Grütter, M. G., Weaver, L. H. & Mathews, B. W. (1983). Goose lysozyme structure – an evolutionary link between hen and bacteriophage lysozymes. *Nature,* **303**, 828–831.

Hart, P. J., Pfluger, H. D., Monzingo, A. F., Hollis, T. & Robertus, J. D. (1995). The refined crystal structure of an endochitinase from *Hordeum vulgare* seeds at 1.8 Å resolution. *J. Mol. Biol.* **248**, 402–413.

Henrissat, B. & Bairoch, A. (1993). New families in the classification of glycosyl hydrolases based on amino acid sequence similarities. *Biochem. J.* **293**, 781–788.

Iseli, B., Armand, S., Boller, T., Neuhaus, J.-M. & Henrissat, B. (1996). Plant chitinases use two different hydrolytic mechanisms. *FEBS Letters,* **382**, 186–188.

Kinoshita, M., Sakuda, S. & Yamada, Y. (1993). Preparation of *N*-monoalkyl and *O*-acyl derivatives of allosamidin, and their chitinase inhibitory activities. *Biosci. Biotech. Biochem.* **57**, 1699–1703.

Koga, D., Isogai, A., Sakuda, S., Matsumato, S., Suzuki, A., Kimura, S. & Ide, A. (1987). Specific inhibition of *Bombyx mori* chitinase by allosamidin. *Agric. Biol. Chem.* **51**, 471–476.

Koshland, D. E. (1953). Stereochemistry and the mechanism of enzymatic reactions. *Biol. Rev.* **28**, 416–436.

Langlois, J.-M., Yamasaki, T., Muller, R. P. & Goddard, W. A., III (1994). Rule-based trial wave-functions for generalized valence-bond theory. *J. Phys. Chem.* **98**, 13498–13505.

Lowe, G., Sheppard, G., Sinnot, M. L. & Williams, A. (1967). Lysozyme-catalysed hydrolysis of some β-aryl di-*N*-acetylchitobiosides. *Biochem. J.* **104**, 893–899.

Mayo, S. L., Olafson, B. D. & Goddard, W. A., III (1990). DREIDING: a generic force-field for molecular simulations. *J. Phys. Chem.* **94**, 8897–8909.

McCarter, J. D. & Withers, S. G. (1994). Mechanisms of enzymatic glycoside hydrolysis. *Curr. Opin. Struct. Biol.* **4**, 885–892.

Muller, R. P., Langlois, J.-M., Ringnalda, M. N., Friesner, R. A. & Goddard, W. A., III (1994). A generalized direct inversion in the interative subspace approach for generalized valence-bond wavefunctions. *J. Chem. Phys.* **100**, 1226–1235.

Murphy, R. B., Friesner, R. A., Ringnalda, M. N. & Goddard, W. A., III (1994). Pseudospectral contracted configuration-interaction from a generalized valence-bond reference. *J. Chem. Phys.* **101**, 2986–2994.

Parsons, S. M. & Raferty, M. A. (1969). The identification of aspartic acid residue 52 as being critical to lysozyme activity. *Biochemistry,* **8**, 4199–4205.

Perrakis, A., Tews, I., Dauter, Z., Oppenheim, A. B., Chet, I., Wilson, K. S. & Vörgias, C. E. (1994). Crystal structure of a bacterial chitinase at 2.3 Å resolution. *Structure,* **2**, 1169–1180.

Phillips, D. C. (1967). The hen egg-white lysozyme molecule. *Proc. Natl Acad. Sci. USA,* **57**, 484–495.

Piszkiewiez, D. & Bruice, T. C. (1967). Glycoside hydrolysis. I. Intramolecular acetamido and hydroxyl group catalysis in glycoside hydrolysis. *J. Am. Chem. Soc.* **89**, 6237–6243.

Piszkiewiez, D. & Bruice, T. C. (1968). Glycoside hydrolysis. II. Intramolecular carboxyl and acetamido group catalysis in β-glycoside hydrolysis. *J. Am. Chem. Soc.* **90**, 2156–2163.

Robertus, J. D., Hart, P. J., Monzingo, A. F., Marcotte, E. & Hollis, T. (1995). The structure of chitinases and prospects for structure-based drug design. *Can. J. Bot.* **73**, S1142–S1146.

Sakuda, S., Isogai, A., Matsumoto, S. & Suzuki, A. (1986). The structure of allosamidin, a novel insect chitinase inhibitor produced by *Streptomyces sp. Tetrahedron Letters,* **27**, 2475–2478.

Schlumbaum, A., Mauch, F., Vögeli, U. & Boller, T. (1986). Plant chitinases are potent inhibitors of fungal growth. *Nature,* **324**, 365–367.

Sinnott, M. L. (1990). Catalytic mechanisms of enzymatic glycosyl transfer. *Chem. Rev.* **90**, 1171–1202.

Tannor, D. J., Marten, B., Murphy, R., Friesner, R. A., Sitkoff, D., Nicholls, A., Ringnalda, M., Goddard, W. A., III & Honig, B. (1994). Accurate first principles calculation of molecular charge-distributions and solvation energies from *ab initio* quantum-mechanics and continuum dielectric theory. *J. Am. Chem. Soc.* **116**, 11875–11882.

Terwisscha van Scheltinga, A. C., Kalk, K. H., Beintema, J. J. & Dijkstra, B. W. (1994). Crystal structures of hevamine, a plant defence protein with chitinase and lysozyme activity, and its complex with an inhibitor. *Structure,* **2**, 1181–1189.

Terwisscha van Scheltinga, A. C., Armand, S., Kalk, K. H., Isogai, A., Henrissat, B. & Dijkstra, B. W. (1995). Stereochemistry of chitin hydrolysis by a plant chitinase/lysozyme and X-ray structure of a complex with allsoamidin: evidence for substrate assisted catalysis. *Biochemistry,* **34**, 15619–15623.

Terwisscha van Scheltinga, A. C., Hennig, M. & Dijkstra, B. W. (1996). The 1.8 Å resolution structure of hevamine, a plant chitinase/lysozyme, and analysis of the conserved sequence and structure motifs

of glycosyl hydrolase family 18. *J. Mol. Biol.* **262**, 243–257.
Thunnissen, A.-M. W. H., Dijkstra, A. J., Kalk, K. H., Rozeboom, H. J., Engel, H., Keck, W. & Dijkstra, B. W. (1994). Doughnut-shaped structure of a bacterial muramidase revealed by X-ray crystallography. *Nature*, **367**, 750–753.
Thunnissen, A.-M. W. H., Rozeboom, H. J., Kalk, K. H. & Dijkstra, B. W. (1995). Structure of the 790-kDa soluble lytic transglycosylase complexed with bulgecin A. Implications for the enzymatic mechanism. *Biochemistry*, **34**, 12729–12737.
Van Vranken, D. L. (1992). pp. 8–9, PhD thesis, Synthesis of aminohydroxy-glycosidase inhibitors and enantioselective palladium catalysis (Volumes I and II). Stanford University.
Warshel, A. & Levitt, M. (1976). Theoretical studies of enymic reactions: dielectric, electrostatic and steric stabilization of the carbonium ion in the reaction of lysozyme. *J. Mol. Biol.* **103**, 227–249.
Weaver, L. H., Grütter, M. G. & Mathews, B. W. (1995). The refined structures of goose lysozyme and its complex with a bound trisaccharide show that the ''goose-type'' lysozymes lack a catalytic aspartate residue. *J. Mol. Biol.* **245**, 54–68.

Edited by B. Honig

(Received 24 March 1998; accepted 30 March 1998)

http://www.hbuk.co.uk/jmb

Supplementary material comprising two Tables is available from JMB Online.